Development 133, 3473-3484 (2006) doi:10.1242/dev.02499

Bone morphogenetic protein receptor 1A signaling is dispensable for hematopoietic development but essential for vessel and atrioventricular endocardial cushion formation

Changwon Park[1,2], Kory Lavine[3], Yuji Mishina[4], Chu-Xia Deng[5], David M. Ornitz[3] and Kyunghee Choi[1,2,*]

Bone morphogenetic protein 4 (BMP4) is crucial for the formation of FLK1-expressing (FLK1$^+$) mesodermal cells. To further define the requirement for BMP signaling in the differentiation of blood, endothelial and smooth muscle cells from FLK1$^+$ mesoderm, we inactivated *Alk3* (*Bmpr1a*) in FLK1$^+$ cells by crossing *Alk3*$^{floxed/floxed}$ and *Flk1*$^{+/Cre}$*Alk3*$^{+/floxed}$ mice. *Alk3* conditional knockout (CKO) mice died between E10.5 and E11.5. Unexpectedly, *Alk3* CKO embryos did not show any hematopoietic defects. However, *Alk3* CKO embryos displayed multiple abnormalities in vascular development, including vessel remodeling and maturation, which contributed to severe abdominal hemorrhage. *Alk3* CKO embryos also displayed defects in atrioventricular canal (AVC) endocardial cushion formation in the heart. Collectively, our studies indicate a crucial role for ALK3 in vessel remodeling, vessel integrity and endocardial cushion formation during the development of the circulation system.

KEY WORDS: Hematopoiesis, Vasculogenesis, Endocardial cushion, FLK1 (KDR), ALK3 (BMPR1A), SMAD4, Mouse

INTRODUCTION

The establishment of the circulatory system including blood, vasculature and the heart is highly coordinated and a prerequisite for embryonic development. A failure of proper development in any of these cell lineages leads to embryonic lethality. Recent studies have established that cells of the circulatory system develop from FLK1$^+$ mesoderm. FLK1 (KDR – Mouse Genome Informatics) is a receptor tyrosine kinase that binds vascular endothelial growth factor (VEGF). In primitive streak stage embryos, *Flk1* expression is first detectable in the extra-embryonic mesoderm and in the paraxial-lateral embryonic mesoderm (Yamaguchi et al., 1993). Subsequently, its expression is confined to endothelial cells and to the developing endocardial tube. Consistent with this expression pattern, *Flk1*-deficient mice die between E8.5 and E9.5 with defects in yolk-sac blood-island formation and vasculogenesis (Shalaby et al., 1995). Cell replating and transplantation experiments have demonstrated that FLK1$^+$ cells isolated from differentiated embryonic stem (ES) cells or embryos generate hematopoietic, endothelial and vascular smooth muscle cells. For example, ES- and embryo-derived FLK1$^+$ cells, but not FLK1$^-$ cells, are enriched for blast colony forming cells (BL-CFCs), an in vitro equivalent of the hemangioblast (Chung et al., 2002; Faloon et al., 2000; Huber et al., 2004). Ema et al. (Ema et al., 2003) showed that BL-CFCs are multipotential, such that blast colonies from single FLK1$^+$ cells could generate smooth muscle cells, as well as hematopoietic and endothelial cells in vitro. Similarly, Yamashita et al. (Yamashita et al., 2000) reported that FLK1$^+$ cells could generate both smooth muscle and endothelial cells in vitro and in vivo. Subsequent fate-mapping studies of FLK1$^+$ cells by using *Flk1*$^{+/Cre}$ and Rosa26-LacZ reporter (R26R) mice showed that FLK1$^+$ cells could also contribute to cardiac and skeletal muscle (Motoike et al., 2003). Collectively, these studies indicate that FLK1$^+$ mesoderm generates cells of the circulation system.

Using the in vitro differentiation model of ES cells, we recently showed that BMP4 was able to induce FLK1$^+$ cells (Park et al., 2004). In serum-free conditions, BMP4 activated the SMAD1/5 pathway. Inhibition of the SMAD1/5 pathway reduced the generation of FLK1$^+$ cells. Consistent with the notion that BMP4 is crucial for the generation of FLK1$^+$ mesoderm, *Bmp4*-deficient mice die between E6.5 and E9.5 with defects in mesoderm formation and patterning. Those that survive up to E9.5 show severe defects in blood islands (Winnier et al., 1995). Additionally, mice lacking the BMP receptor type IA (ALK3; BMPR1A – Mouse Genome Informatics) fail to complete gastrulation, and none survive past the E9.5 stage (Mishina et al., 1995). *Smad1*-deficient mice display early embryonic lethality and die between E9.5 and E10.5 owing to the failure of chorioallantoic fusion (Lechleider et al., 2001; Tremblay et al., 2001). *Smad5*-deficient mice die between E9.5 and E11.5, displaying anemia and disorganized vessels, despite the formation of the primitive vascular plexus (Chang et al., 1999; Yang et al., 1999). Collectively, these studies have shed light on BMPs and their downstream signaling in embryonic development. However, the early lethality with complex abnormalities precludes placing the precise window in which they play a role in hematopoietic and endothelial cell development.

To better understand the requirement of BMP signaling in blood and endothelial cell development, we inactivated *Alk3* in FLK1$^+$ mesoderm by using *Flk1*$^{+/Cre}$ knock-in mice. Our studies demonstrate an essential role for signaling through ALK3 in vessel remodeling and maturation. Mutant embryos died between E10.5 and E11.5, with defects in vessel remodeling and smooth muscle cell formation and/or recruitment to the dorsal aorta. Mutant embryos also displayed defects of endocardial cushion formation in the AVC. We propose that ALK3 signaling in FLK1$^+$ mesoderm is crucial for proper vessel formation and heart development.

[1]Department of Pathology and Immunology, Washington University School of Medicine, 660 South Euclid, St Louis, MO 63110, USA. [2]Developmental Biology Program, Washington University School of Medicine, 660 South Euclid, St Louis, MO 63110, USA. [3]Department of Molecular Biology and Pharmacology, Washington University School of Medicine, 660 South Euclid, St Louis, MO 63110, USA. [4]Molecular Developmental Biology Group, National Institute of Environmental Health Sciences, Research Triangle Park, NC 27709, USA. [5]Genetics of Development and Disease Branch, NIDDK, NIH, Bethesda, MD 20892, USA.

*Author for correspondence (e-mail: kchoi@wustl.edu)

Accepted 16 June 2006

MATERIALS AND METHODS

Generation of mouse lines

To generate FLK1$^+$ cell-specific *Alk3* or *Smad4* CKO mice, *Alk3$^{floxed/floxed}$* or *Smad4$^{floxed/floxed}$* mice were crossed with *Flk1$^{+/Cre}$Alk3$^{+/floxed}$* or *Flk1$^{+/Cre}$Samd4$^{+/floxed}$* mice, respectively. *Flk1$^{+/Cre}$* mice (a gift of Dr Sato at the University of Southwestern Medical School, TX) were made by a knock-in strategy wherein Cre recombinase is expressed under the control of the endogenous *Flk1* promoter (Motoike et al., 2003). The generation of *Alk3$^{floxed/floxed}$* and *Smad4 $^{floxed/floxed}$* mice and genotyping were previously described (Mishina et al., 2002; Yang et al., 2002).

Histological analysis

Embryos were fixed in 4% paraformaldehyde (PFA), paraffin embedded and sagittally sectioned at 5 μm. For antigen retrieval, sections on the slides were incubated with 0.1% trypsin for 15 minutes at 37°C and washed with phosphate-buffered saline (PBS). The sections were immersed in blocking buffer (5% normal goat serum and 0.1% Tween 20 in PBS) for 40 minutes at room temperature, followed by overnight incubation at 4°C with anti-PECAM1 antibody (1:30, Pharmingen). After incubation with anti-biotinylated rat IgG (1:200, Zymed), the sections were further incubated with anti-SMC actin antibody (1:200, Sigma) and Cy5-conjugated streptavidin (1:400). For cross-sections, frozen cryosections of 10 μm were stained with antibodies as described above without an antigen retrieval step.

Whole-mount staining

Embryos were fixed overnight in Dent's fixative (methanol and DMSO, 4:1) at 4°C, followed by blocking in PBS containing 5% normal goat serum, 0.1% Tween 20 and 2% non-fat skim milk) for 2 hours at room temperature. After incubation with anti-PECAM1 antibody (1:300) and alkaline phosphatase-conjugated anti-Rat IgG (1:250, Zymed), signals were detected with the NBT/BCIP kit (Promega). For yolk sac, 4% PFA was used instead of Dent's fixative, blocking and antibody incubation were performed in PBS containing 5% normal goat serum and 1% DMSO (Morikawa and Cserjesi, 2004).

Real time quantitative reverse transcription PCR

RNAs from tissues were extracted by using Trizol (Gibco). cDNA was generated using the Invitrogen kit. Expression of genes indicated in the text was measured by real-time qRT-PCR, and normalized by *Gapdh* expression. Each experiment with duplicates was performed at least three times. For primers, see Table 1.

Transmission electron microscopy

For ultrastructural analysis, embryos were fixed in 2% PFA/2.5% glutaraldehyde (Polysciences, Warrington, PA) in 100 mM phosphate buffer (pH 7.2) overnight at 4°C followed by post fixation in 1% osmium tetroxide (Electron Microscopy Sciences, Fort Washington, PA) for 1 hour. Osmium tetroxide was removed and samples were stored in 100 mM phosphate buffer at 4°C pending genotype analysis. Samples were then rinsed extensively in distilled H_2O to remove excess phosphate prior to en bloc staining with 1% aqueous uranyl acetate (Ted Pella, Redding, CA) for 1 hour. Samples were washed, dehydrated in a graded series of ethanol, and embedded in Eponate 12 resin (Ted Pella). Sections of 95 nm were cut, stained with uranyl acetate and lead citrate and viewed on a JEOL 1200 EX transmission electron microscope (JEOL USA, Peabody, MA).

Hematopoietic colony assay

Hematopoietic colonies were generated as described previously (Faloon et al., 2000; Palis et al., 1999). Briefly, yolk sacs were isolated, dissociated in collagenase with 20% FBS, and the resulting cells were replated in 1% methyl cellulose containing hematopoietic cytokines. The dissociated fetal liver cells from E10.5 embryos were replated in Methocult M3434 (Stemcell Tech, CA). Hematopoietic colonies were counted 4-7 days later.

Statistics

The results of real-time quantitative reverse transcription PCR were analyzed by Student's *t*-test. $P<0.05$ was considered significant.

RESULTS

Establish *Alk3* conditional knockout mice

To inactivate *Alk3* in FLK1$^+$ cells, we employed two mouse lines, *Alk3$^{floxed/floxed}$* mice, in which exon 2 is flanked by loxP sites (Mishina et al., 2002) and *Flk1$^{+/Cre}$* mice, in which the *Cre* gene is introduced into one allele of the *Flk1* locus (Motoike et al., 2003). The expression of Cre recombinase in these mice is under the control of the endogenous *Flk1* promoter, providing the specific deletion of floxed genes in FLK1$^+$ cells. To generate *Alk3* CKO mice, we first set up matings between *Flk1$^{+/Cre}$* and *Alk3$^{floxed/floxed}$* mice. *Flk1$^{+/Cre}$Alk3$^{+/floxed}$* mice were subsequently mated with *Alk3$^{floxed/floxed}$* mice to generate *Flk1$^{+/Cre}$Alk3$^{floxed/floxed}$* CKO mice (Fig. 1A). The expected ratio of obtaining *Alk3$^{floxed/floxed}$*, *Alk3$^{+/floxed}$*,

Table 1. Primer sequences for qRT-PCR

GAPDH	Sense	5′-TGGCAAAGTGGAGATTGTTGCC-3′	Antisense	5′-AAGATGGTGATGGGCTTCCCG-3′
ID1	Sense	5′-CATGAACGGCTGCTACTCAC-3′	Antisense	5′-GTGGTCCCGACTTCAGACTC-3′
ID2	Sense	5′-CCCGATGAGTCTGCTCTACA-3′	Antisense	5′-GCAGGTCCAAGATGTAATCG-3′
ID3	Sense	5′-CAGCTTAGCCAGGTGGAAAT-3′	Antisense	5′-AGTGAGCTCAGCTGTCTGGA-3′
ID4	Sense	5′-GAGGCTCGTGCCTACCATC-3′	Antisense	5′-CTCAGCAAAGCAGGGTGAGT-3′
SMC α-actin	Sense	5′-GAACGCTTCCGCTGCCC-3′	Antisense	5′-GGATGCCCGCTGACTCC-3′
SMC α-MHC	Sense	5′-CATGGACCCGCTAAATGACA-3′	Antisense	5′-CAATGCGGTCCACATCCTTC-3′
CD31	Sense	5′-GAGCCCAATCACGTTTCAGTTT-3′	Antisense	5′-TCCTTCCTGCTTCTTGCTAGCT-3′
Angiopoietin 1	Sense	5′-CTCGTCAGACATTCATCATCCAG-3′	Antisense	5′-CACCTTCTTTAGTGCAAAGGCT-3′
TIE2	Sense	5′-GACGATTTACAAACAGCGTCTATCGG-3′	Antisense	5′-GGGAGAATGTCACTAAGGGTCCAG-3′
VEGF	Sense	5′-CATAGAGAGAATGAGCTTCCTACAGC-3′	Antisense	5′-TGCTTTCTCCGCTCTGAACAAGG-3′
PTEN	Sense	5′-AAAGGGACGGACTGGTGTAA-3′	Antisense	5′-CCTCTGACTGGGAATTGTGA-3′
Integrin αV	Sense	5′-GTTTGATTCAACAGGCAATCGAG-3′	Antisense	5′-CAGGCCAAGATTTTATCCTGCTT-3′
Integrin β3	Sense	5′-TCTGGGTAATAGGACTCCGAGA-3′	Antisense	5′-GTTTGATTCAACAGGCAATCGAG-3′
SNAI1	Sense	5′-CACACGCTGCCTTGTGTCT-3′	Antisense	5′-GGTCAGCAAAAGCACGGTT-3′
VE-cadherin	Sense	5′-TCCTCTGCATCCTCACTATCACA-3′	Antisense	5′-GTAAGTGACCAACTGCTCGTGAAT-3′
SOX9	Sense	5′-ACGGCTCCAGCAAGAACAAG-3′	Antisense	5′-TTGTGCAGATGCGGGTACTG-3′
NFATC1	Sense	5′-CCCGTTGCTTCCAGAAAATA-3′	Antisense	5′-TCTTCCTCCCGATGTCTGTC-3′
TGFβ2	Sense	5′-GCAAGGTTGTGAAAACCAGA-3′	Antisense	5′-TAGACGGCACGAAGGTACAG-3′
MSX1	Sense	5′-CCAGGTGAAGATCTGGTTCC-3′	Antisense	5′-CAGGAAAAGAGAGGCCGAAG-3′
TWIST1	Sense	5′-ACGCAGTCGCTGAACGAGGC-3′	Antisense	5′-GTACAGGAAGTCGATGTACC-3′
uPA	Sense	5′-CTGCCCAAGGAAATTCCAGGG-3′	Antisense	5′-ACCTTTGGTATCAGTGTTGGC-3′
PLAU1	Sense	5′-TTCGGAGTAAAAGTGTTTCAGCA-3′	Antisense	5′-TGAGCTGTGCCCTTCTCATTG-3′

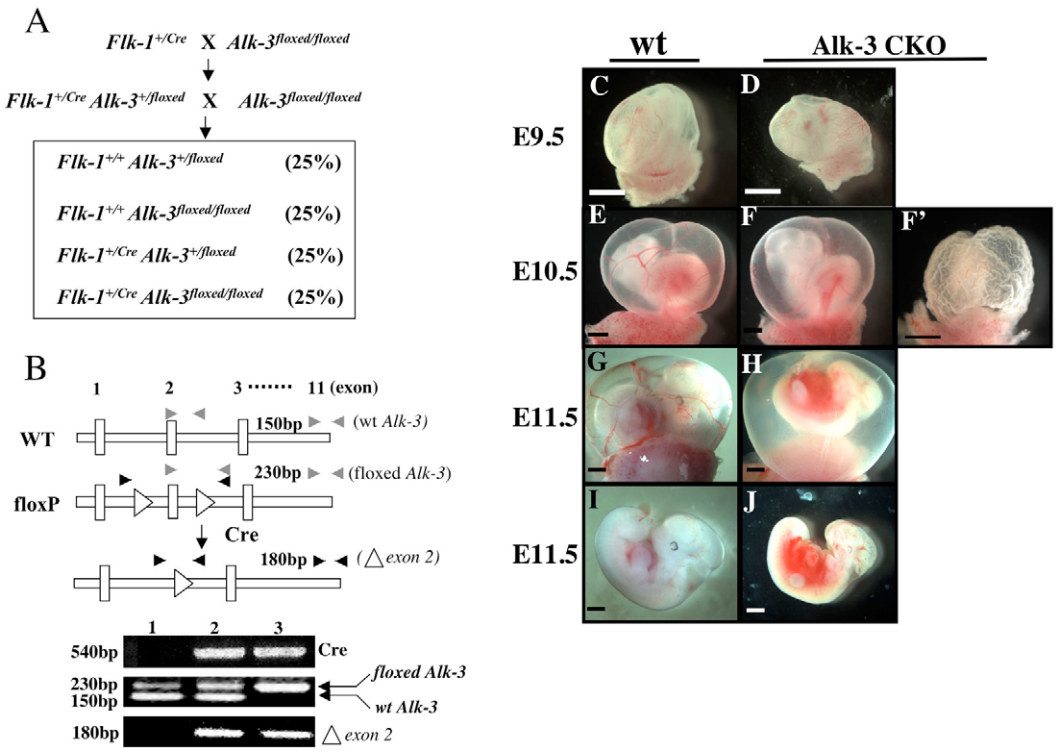

Fig. 1. Generation of *Flk1*$^{+/Cre}$*Alk3*$^{floxed/floxed}$ mice. (**A**) The mating scheme used to generate *Alk3* CKO and control littermates. (**B**) (Upper) A 150 bp fragment from wild-type *Alk3* allele and a 230 bp fragment from floxed *Alk3* allele can be PCR-amplified with primers indicated by gray triangles (sense, 5′-GCAGCTGCTGCTGCAGCCTCC-3′; antisense, 5′-TGGCTACAATTTGTCTCATGC-3′). A 180 bp fragment should appear with primers indicated by black triangles (sense, 5′-GGTTTGGATCTTAACCTTAGG-3′; antisense, 5′-TGGCTACAATTTGTCTCATGC-3′) if Cre–mediated recombination occurs. The presence of the knock-in *Cre* gene was confirmed by a 540 bp fragment using: sense, 5′-GAAACCGAGCTGCGTCCAGATTT-3′; antisense, 5′-GGTGTACGGTCAGTAAATTGG-3′. (Lower) A representative tail genomic DNA PCR results. Lane 1, *Alk3*$^{+/floxed}$; lane 2, *Flk1*$^{+/Cre}$*Alk3*$^{+/floxed}$; lane 3, *Flk1*$^{+/Cre}$*Alk3*$^{floxed/floxed}$. (**C-J**) Gross morphology of *Alk3* CKO embryos. Scale bars: 1 mm.

Flk1$^{+/Cre}$*Alk3*$^{+/floxed}$, *Flk1*$^{+/Cre}$*Alk3*$^{floxed/floxed}$ mice is 1:1:1:1, respectively. Genomic DNA PCR was used to verify the expected genotypes (Fig. 1B).

Alk3 inactivation within FLK1 expressing cells results in embryonic lethality

We initially analyzed 147 pups at 3-4 weeks of age. As shown in Table 2, no live *Flk1*$^{+/Cre}$*Alk3*$^{floxed/floxed}$ (*Alk3* CKO) pups were detected, although mice with all three other potential genotypes were present. This indicated that inactivation of *Alk3* in FLK1^{+} mesoderm caused embryonic lethality. To identify the stage at which embryos died, we examined embryos obtained from scheduled matings. *Alk3* CKO embryos were morphologically indistinguishable from control embryos at E9.5 (Table 1 and Fig. 1D). However, at E10.5, 21 out of 69 *Alk3* CKO embryos were moribund and displayed pale yolk sacs (Table 2 and Fig. 1F′). The remaining 48 *Alk3* CKO embryos were morphologically indistinguishable from wild-type embryos (Fig. 1F). At E11.5, all *Alk3* CKO embryos had pale yolk sacs and showed hemorrhage throughout the trunk region of the embryo (Fig. 1H,J). The mutant hearts were smaller than those of the control embryos, and the cavity between the pericardial sac and the heart was distended in the mutant embryos (not shown). At E12.5, *Alk3* CKO embryos were totally pale, although some of them still had red fluid within the amnion (not shown). The mutants were much smaller than the controls, and digit formation did not occur in these mutants, indicating that they failed to develop beyond E11.5. These initial observations indicated that *Alk3* CKO embryos died between E10.5 and E11.5, and suggested that they had defects in the circulatory system.

Normal hematopoiesis in *Alk3* CKO embryos

As BMP4/SMAD1/5 signaling has been implicated to be crucial for hematopoietic development (Chang et al., 1999; Johansson and Wiles, 1995; Kanatsu and Nishikawa, 1996; Liu et al., 2003; Park

Table 2. Genotypic analysis of pups from *Flk1*$^{+/Cre}$*Alk3*$^{+/floxed}$ × *Alk3*$^{floxed/floxed}$

	Flk1$^{+/Cre}$*Alk3*$^{floxed/floxed}$	*Flk1*$^{+/Cre}$*Alk3*$^{+/floxed}$	*Alk3*$^{floxed/floxed}$	*Alk3*$^{+/floxed}$
E9.5	25(1*)/101	28/101	27/101	21/101
E10.5	69(21*)/274	53(4*)/274	78/274	74(2*)/274
E11.5	10*/36	8/36	8/36	10/36
E12.5	5*/30	5/30	8/30	12/30
E13.5	1*/13	4*/13	4/13	4/13
P21	0/147	40/147	52/147	55/147

E, embryonic day; P, postnatal day; *, number of moribund embryos.

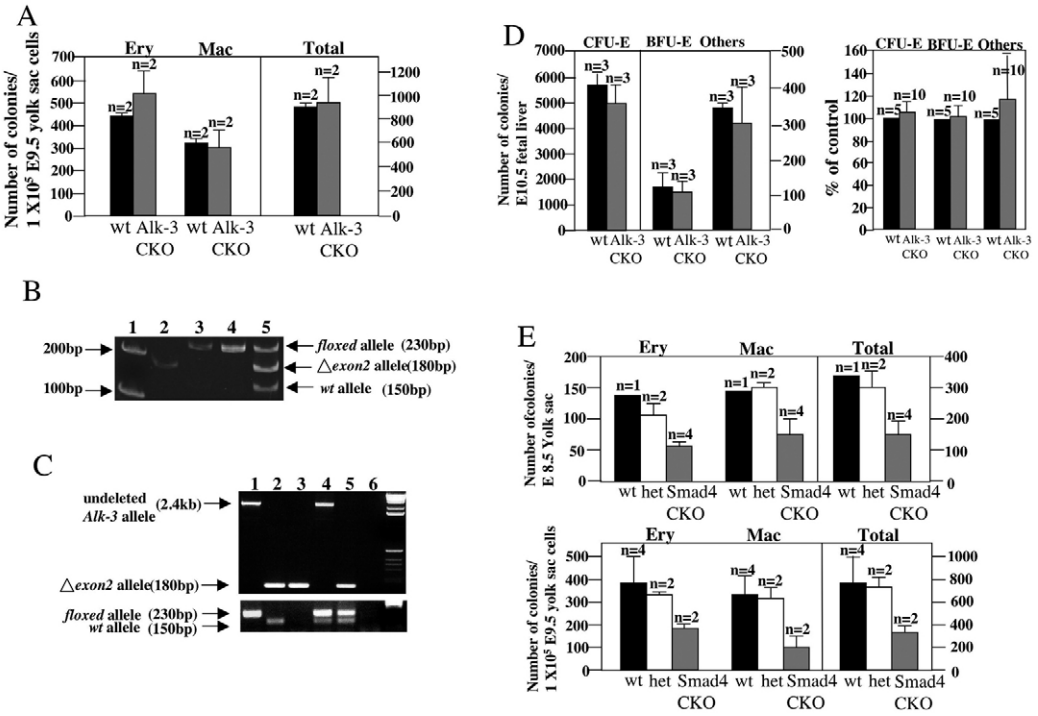

Fig. 2. Hematopoietic potential of *Alk3* CKO and *Smad4* CKO embryos. E9.5 *Alk3* CKO yolk sacs (**A**), E10.5 fetal liver (**D**), *Smad4* CKO yolk sacs (**E**; upper, E8.5; lower, E9.5) were dissociated and plated into methylcellulose cultures with hematopoietic cytokines. Four to seven days later, colonies were counted and plotted. Bar indicates the average number of colonies; error bars indicate standard deviations; n, number of embryos. One representative result is shown. Similar results were obtained from three independent experiments. Ery, erythrocytes; Mac, macrophage, CFU-E, colony forming unit-erythrocyte; BFU-E, burst forming unit-erythrocyte. (**B**) Genomic PCR of sorted FLK1$^+$ or TER119$^+$ cells in E9.5 yolk sacs. Lane 1, molecular marker; lane 2, sorted cells from *Flk1*$^{+/Cre}$*Alk3*$^{floxed/floxed}$; lane 3, sorted cells from *Alk3*$^{floxed/floxed}$; lane 4; whole yolk sac cells from *Alk3*$^{floxed/floxed}$; lane 5, whole yolk sac cells from *Flk1*$^{+/Cre}$*Alk3*$^{+/floxed}$. (**C**) Genomic PCR on hematopoietic colonies grown from E9.5 *Alk3* CKO yolk sac replating. Lane 1, *Alk3*$^{floxed/floxed}$; lane 2, *Flk1*$^{+/Cre}$*Alk3*$^{+/floxed}$; lane 3, *Flk1*$^{+/Cre}$*Alk3*$^{floxed/floxed}$; lane 4, *Alk3*$^{+/floxed}$; lane 5, positive control; lane 6, Negative control (H_2O).

et al., 2004), it was expected that *Alk3* CKO embryos might display defects in hematopoiesis. Initial observation of the E9.5 mutants, however, indicated that red blood cells were present (Fig. 1D). To determine if the level of hematopoietic progenitors present in the mutant yolk sacs was diminished, we performed hematopoietic progenitor assays. Yolk sacs from E9.5 embryos were isolated, dissociated and plated into methylcellulose supplemented with hematopoietic cytokines. As shown in Fig. 2A, similar numbers of erythroid and macrophage colonies developed from the *Alk3* CKO and control yolk sacs. The hematopoietic colonies that developed from the *Alk3* CKO yolk sacs were confirmed by Giemsa staining (not shown). To determine whether incomplete *Alk3* deletion could have resulted in the generation of hematopoietic colonies from the *Alk3* CKO yolk sac, FLK1$^+$ cells or TER119$^+$ (LY76$^+$ – Mouse Genome Informatics) cells (erythrocytes) from E9.5 yolk sacs were FACS sorted and subjected to genomic PCR. As shown in Fig. 2B, the correctly excised band was detectable in DNA obtained from the *Alk3* CKO yolk sac-derived FLK1$^+$ cells or TER119$^+$ cells. By densitometry, we estimated that over 95% of the floxed exon 2 was correctly deleted in the *Alk3* CKO cells. Moreover, when the *Alk3* CKO yolk sac-derived hematopoietic colonies were picked and subjected to genomic PCR, a PCR band corresponding to the floxed exon 2 of *Alk3* was present in the controls, but not in the mutants, demonstrating that *Alk3* was correctly deleted in all mutant-derived hematopoietic colonies (Fig. 2C). Previous studies indicate that E9.5 yolk sacs contain predominantly definitive hematopoietic progenitors (Palis et al., 1999). To further validate that definitive hematopoiesis was indeed unaffected in the *Alk3* CKO embryos, we dissected out E10.5 fetal liver and performed hematopoietic colony assays. As shown in Fig. 2D, *Alk3* CKO fetal liver generated a similar number of hematopoietic colonies compared with controls. Collectively, the relatively normal frequency of hematopoietic progenitors present in E9.5 mutant yolk sacs and in E10.5 mutant fetal livers argues that ALK3 signaling is not constitutively required for hematopoietic development.

The finding that *Alk3* CKO embryos showed normal hematopoiesis was rather unexpected, as BMP4 is thought to be crucial for hematopoietic development. To determine whether BMP, TGFβ or activin signaling is involved at all in hematopoietic development, we generated *Smad4* CKO mice by crossing *Smad4*$^{floxed/floxed}$ (Yang et al., 2002) and *Flk1*$^{+/Cre}$*Smad4*$^{+/floxed}$ (see Table S1 and Fig. S1 in the supplementary material). SMAD4 is the common SMAD that mediates signaling by all members of the TGFβ superfamily. *Smad4* CKO mutants died earlier than *Alk3* CKO mutants, between E9.5 and E10.5 (see Table S1 in the supplementary material). Performing a hematopoietic progenitor assay at E8.5 revealed that the number of hematopoietic colonies in *Smad4* CKO embryos was decreased by about 50% compared with controls (Fig. 2E, upper). E9.5 yolk sac replating generated similar results (Fig. 2E, lower). Hematopoietic colonies that developed from the *Smad4* CKO and wild-type yolk sacs were indistinguishable in size and morphology. A complete deletion of floxed exon 8 of *Smad4* was confirmed by genomic PCR on yolk

sac-derived hematopoietic colonies (see Fig. S1 in the supplementary material). Collectively, these studies demonstrate that BMP, TGFβ or activin signaling contributes to hematopoietic differentiation from FLK1$^+$ mesoderm; however, such signaling is not mediated by ALK3.

Defective vessel development in *Alk3* CKO embryos

The *Alk3* CKO mutants that died by E10.5 exhibited anemic yolk sacs (Fig. 1F′). As hematopoiesis was undisturbed, vessel development might be defective. To test this possibility, we analyzed yolk sac vasculature by whole-mount staining using anti-PECAM1 (CD31) antibody, a marker for endothelial cells. As shown, wild-type embryos displayed large vessels with extensive branching and a well-developed capillary network (Fig. 3A). However, *Alk3* CKO E10.5 yolk sacs showed only the primary vascular plexus of poorly developed vascular channels (Fig. 3B). Similarly, abnormal CD31 staining was obvious in the *Alk3* CKO mutant brain vasculature (Fig. 3D). From these observations, we conclude that ALK3 is required for vessel remodeling.

To better understand the molecular mechanisms involved in ALK3-mediated vessel remodeling, we examined the expression of members of the Id family (inhibitor of DNA binding/differentiation). Id genes are important for angiogenesis and are well-known direct downstream targets of BMP signaling (reviewed by Ruzinova and Benezra, 2003). We first evaluated the expression of all Id genes in the yolk sac using quantitative real-time reverse transcription PCR (qRT-PCR). As shown in Fig. 3E, *Id2* was expressed at high levels in E8.5-E10.5 yolk sac, while *Id4* was the least expressed. Importantly, the expression of all Id genes in *Alk3* CKO yolk sacs was decreased by ~40-60% compared with control yolk sacs, suggesting that Id genes are downstream targets of ALK3 signaling in mediating vessel remodeling (Fig. 3F). Additionally, we observed that the expression of urokinase-type plasminogen activator (*Plau*) and peptidase inhibitor 1 (*Serpine1*), both of which are important mediators of angiogenesis, was upregulated in *Alk3* CKO yolk sacs (Fig. 3F).

Alk3 CKOs that survived to E11.5 were morphologically normal at E10.5, but subsequently succumbed to death displaying abdominal hemorrhage (Fig. 1H,J). To further characterize the mutant phenotype, E10.5 wild-type and *Alk3* CKO embryos (excluding those that showed the pale yolk sac phenotype) were subjected to whole-mount CD31 staining. Overall, the mutant embryos did not display distinct abnormalities in CD31 staining in the yolk sac and embryo proper (not shown). Id gene expression in these *Alk3* CKO mutant yolk sacs was comparable with that of the controls (not shown). Nonetheless, they often showed dilated vessels in the brain and abnormal branching in the trunk, confirming a defect in angiogenesis (Fig. 4B,D). As they all displayed abdominal hemorrhage, we reasoned that the vessel integrity could also be defective in these mutants. To explore this possibility, E10.5 wild-type and *Alk3* CKO embryos (excluding those that showed the pale yolk sac phenotype) were sectioned and subjected to immunostaining with anti-CD31 and anti-smooth muscle cell (SMC) α-actin antibody, a marker for vascular SMCs. We examined at least 15 different regions in cross-sections (Fig. 4E-J) and five different regions in sagittal sections (not shown) along the dorsal aorta per embryo. As discussed earlier, mutant embryos appeared to have no obvious defects in vessel structure itself, as judged by CD31 staining (Fig. 4I). However, *Alk3* CKO mutants appeared to have fewer SMCs around the dorsal aorta, compared with wild-type embryos (Fig. 4J). Subsequently, E11.5 dorsal aortas were isolated, RNA was prepared and subjected to qRT-PCR. *Alk3* CKO mutants expressed similar levels of *Cd31* when compared with controls (Fig. 4K, upper panels). However, they all expressed decreased levels of both SMC α-actin and myosin heavy chain (*Mhc*) when compared with the controls, confirming a decreased number of SMCs around the dorsal aorta.

To better characterize the blood vessel defects in *Alk3* CKO embryos, we examined E10.5 wild-type and mutant embryos (excluding those that showed the pale yolk sac phenotype) by transmission electron microscopy (TEM) (Fig. 4L). TEM studies revealed obvious abnormalities in the mutant dorsal aortas. Consistent with SMC α-actin staining and qRT-PCR, the SMC number was diminished. Furthermore, the SMCs that were present did not make close contacts with adjacent endothelial cells. Although we observed relatively normal CD31 staining, there were frequent breaks in the endothelial cell layer in the mutants, while no breaks were found in the wild-type dorsal aortas (Fig. 4L). We further examined genes involved in vessel stability/integrity using the qRT-PCR. Angiopoietin 1 and 2 (*Angpt1* and *Angpt2*), and *Tie2* expression levels were comparable

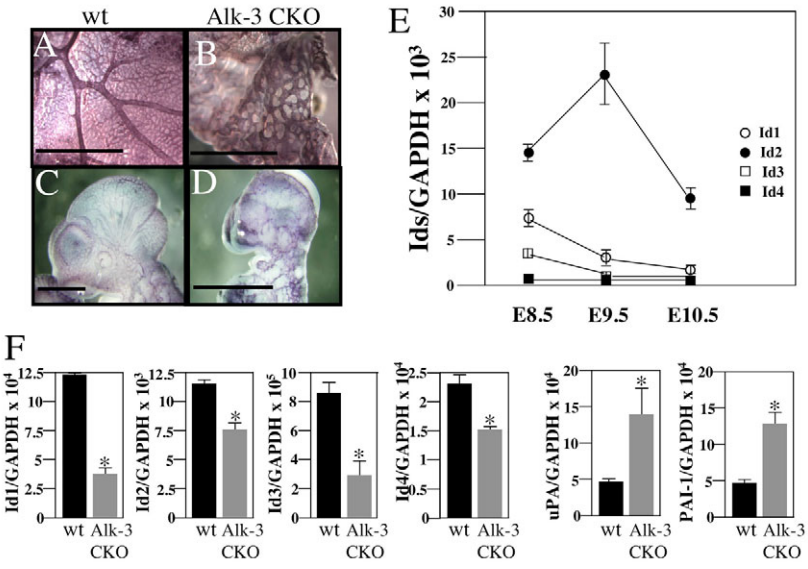

Fig. 3. Vessel remodeling and maturation defect in *Alk3* CKO embryos. Yolk sacs (**A**,**B**) and embryo proper (**C**,**D**) were subjected to whole-mount staining with anti-PECAM1 (CD31) antibodies and were visualized by alkaline phosphatase. The *Alk3* CKO embryos display the primary vascular plexus in yolk sacs (B) and abnormal vascular patterning in the brain (D), but the controls showed normal vasculature pattern (A,C). Scale bars: 1 mm. (**E**) RNAs from E8.5-E10.5 yolk sacs were subjected to qRT-PCR for Id genes (*Id1-Id4*). The relative expression level of *Id1*, *Id2, Id3* and *Id4* in wild-type yolk sacs is shown. (**F**) Expression of all Id genes, *Plau1* and *Serpine1* was examined and compared in the *Alk3* CKO and the controls. RNAs from two wild-type (wt) and two *Alk3* CKO embryos were used for qRT-PCR, respectively. *P<0.05.

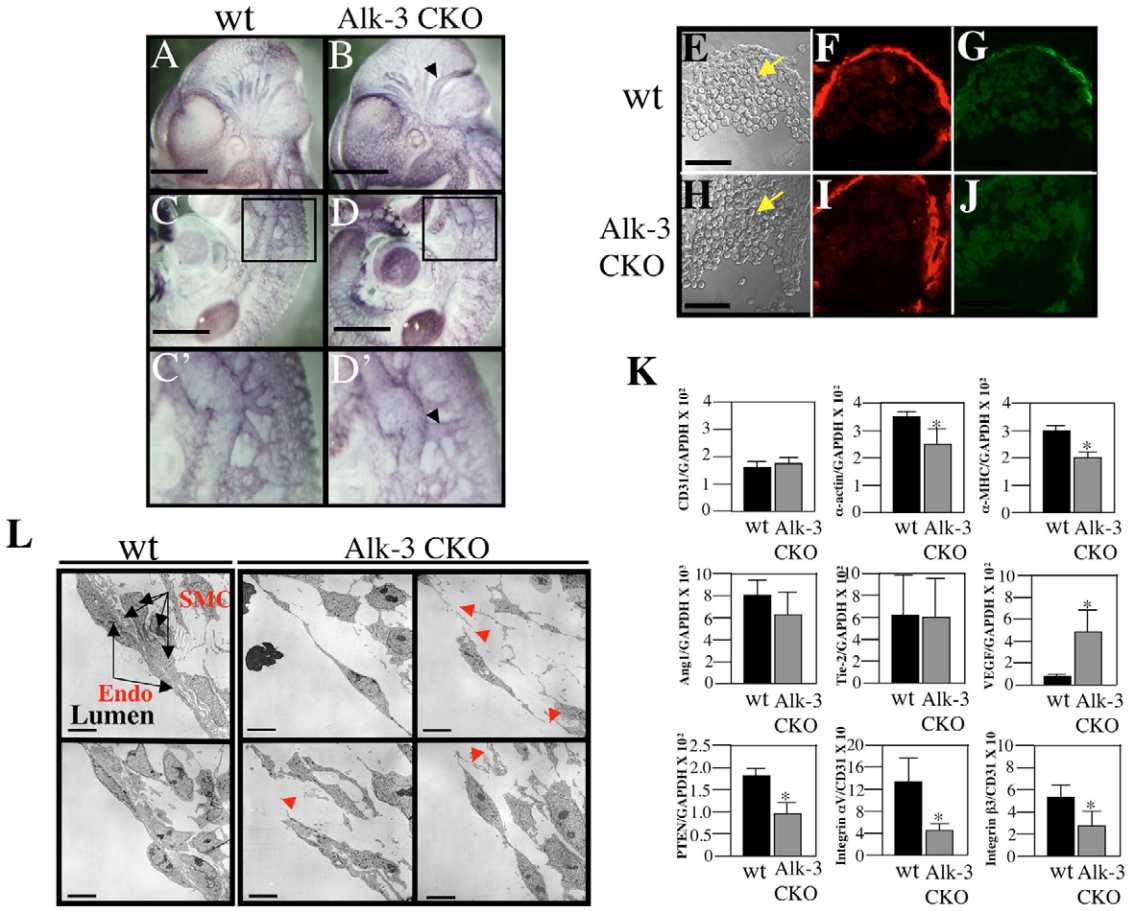

Fig. 4. Disorganized vessel structure in the *Alk3* CKO dorsal aorta. (**A-D'**) Anti-PECAM (CD31) antibody staining. The *Alk3* CKO embryos often exhibited dilated vessels (indicated by arrowheads) in the brain and abnormal patterns of vessel branching in the trunk (B,D,D'), compared with the controls (A,C,C'). (C',D') Higher magnification of the insets of C and D, respectively. Scale bars: 1 mm. (**E-J**) E10.5 embryos were stained with anti-PECAM1 (CD31) antibody (red, F,I) to visualize endothelial cells and anti-SMC α-actin antibody (green, G,J) to visualize SMCs. The endothelial cell layer of the dorsal aorta appeared to be normal, as indicated by anti-CD31 staining in both controls (wild-type) and *Alk3* CKO embryos. SMCs are readily found throughout the dorsal aorta in the controls, but in the mutants SMCs are lacking in some areas of the dorsal aorta. Arrows (E,H) indicate blood cells in the lumen of the dorsal aorta. Three wild-type and three *Alk3* CKO embryos were analyzed in cross-section. Scale bars: 50 μm. (**K**) Quantitative RT-PCR analysis of dorsal aorta for *Cd31*, SMC α-actin, *Mhc*, *Angpt1*, *Tie2*, *Vegf*, *Pten*, integrin αv and integrin β3. Three wild-type and three *Alk3* CKO embryos were used for qRT-PCR. **P*<0.01. (**L**) E10.5 embryos were sectioned and examined under transmission electron microscopy. There are breaks in the *Alk3* CKO dorsal aorta (red arrowheads). In addition, the mutant endothelial cell layer did not form a close association with SMCs, compared with the controls. Two control embryos and four *Alk3* CKO embryos were analyzed for EM study. SMC, smooth muscle cells; Endo, endothelial cells. Scale bars: 6 μm.

between control and *Alk3* CKO embryos (Fig. 4K, middle panels and not shown). However, the expression of integrin αV and β3 was reduced in the mutants, compared with controls (Fig. 4,K lower panels). Importantly, we found decreased expression of *Pten*, but increased expression of *Vegf* in the *Alk3* CKO embryos (Fig. 4K, middle and lower panels). All *Smad4* CKO mutants displayed angiogenesis defects, as only the primary vascular plexus was observed in E9.5 and E10.5 yolk sacs (Fig. 5A). In these *Smad4* CKO yolk sacs, the expression of all Id genes was greatly reduced compared with controls (Fig. 5B). The level of reduction was even greater in *Smad4* CKO yolk sacs compared with *Alk3* CKO yolk sacs. Collectively, we conclude that ALK3, SMAD4 and ID proteins are crucial mediators of vessel remodeling. Moreover, defects in SMC recruitment and/or differentiation, reduced interactions between endothelial cells, and/or increased VEGF could contribute to the abdominal hemorrhage in *Alk3* CKO embryos.

Endocardial cushion defects in *Smad4* and *Alk3* CKO embryos

Previous studies have demonstrated that FLK1$^+$ cells contribute to cardiac muscle as well as endothelial cells and that *Flk1*-deficient mice displayed an endocardial defect (Shalaby et al., 1995). Thus, we examined the hearts of *Smad4* and of *Alk3* CKO embryos by Hematoxylin and Eosin staining. At E9.5, trabeculae in the ventricles and endocardial cushion in the AVC begin to form (Fig. 5C). As shown in Fig. 5D, trabeculae in the ventricles was much thinner and AVC endocardial cushion was not present in *Smad4* CKO hearts. At E10.5, trabeculae develop further and endocardial cushions can be detected in both AVC and outflow track (OFT) (Fig. 6A). When E10.5 *Alk3* CKO hearts (excluding those with the pale yolk sac phenotype) were examined, we detected no cushion cells in the AVC (Fig. 6A). However, development of the OFT cushion appeared to be normal. This observation raised the issue whether FLK1$^+$ cells contribute

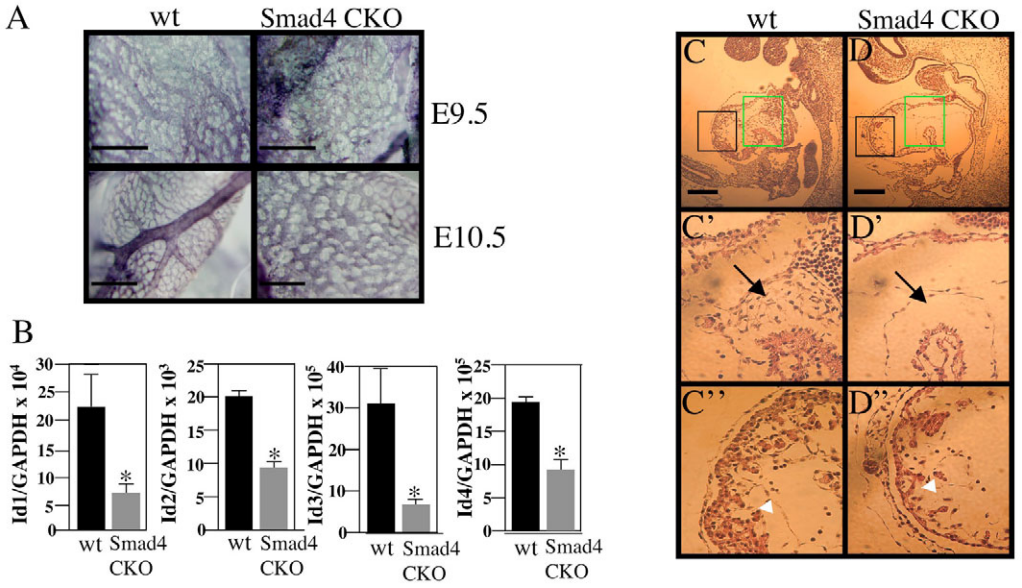

Fig. 5. Defects in vessel remodeling and the heart of the *Smad4* CKO embryos. (**A**) E9.5 and E10.5 yolk sacs of *Smad4* CKO were subjected to whole-mount staining with anti-PECAM1 (CD31) antibody. The controls (wild type) showed complex branching (left), but *Smad4* CKO embryos displayed only the primary vascular plexus (right). Scale bars: 500 μm. (**B**) Expression of Id genes in the *Smad4* CKO yolk sacs. RNAs from two wild-type and three *Smad4* CKO embryos were used for qRT-PCR. **P*<0.05. (**C-D′**) Hematoxylin and Eosin staining of E9.5 heart of *Smad4* CKO embryos. (C′-D″) Higher magnification of the insets (green and black) in C and D, respectively. Arrows indicate the cushion in the AVC and arrowheads indicate the trabeculae in the ventricle. Scale bars: 200 μm.

differently to the cushion cells of the AVC and OFT. To address this, *Flk1*$^{+/Cre}$ mice were crossed with Rosa26R-LacZ mice (Soriano et al., 1999). At E10.5, the majority of *lacZ*-positive cells in the AVC were present in the cushion cell layer and in the endocardium. In the OFT, *lacZ*-positive cells were also found in the endocardium (Fig. 6B). By E12.5, all AVC-cushion cells were *lacZ* positive, while OFT-cushion cells were composed of both *lacZ* positive and negative cells. These results indicate that AVC cushion cells are derived solely from FLK1$^+$ cells, while OFT cushion cells could originate from non-FLK1$^+$ cells, presumably from the neural crest.

To better understand defects in the AVC of the *Alk3* CKO embryos, E10.5 hearts were first stained with Alcian Blue (Fig. 6C). Both wild-type and *Alk3* CKO formed the cardiac jelly, as indicated by blue staining, although the staining pattern and intensity in the *Alk3* CKO mutants appeared to be weaker compared with the wild-type controls. Second, genes important for the EMT were examined. Specifically, E10.5 hearts were dissected free of the OFT and the right ventricle and subjected to gene expression studies. *Alk3* CKO hearts showed a decreased expression of *Snai1* and *Sox9*, but a comparable expression of VE-cadherin and *Nfatc1*, compared with wild-type controls (Fig. 6D). Both *Msx1* and *Twist1* expression was downregulated in the mutant hearts, but *Tgfb2* expression was not changed (Fig. 6D).

DISCUSSION

In this study, we have delineated the function of ALK3 in the differentiation of FLK1$^+$ mesoderm-derived cell lineages, which could not be revealed from the conventional null animals. Specifically, sustained activity of ALK3 is crucial for vessel remodeling, vessel integrity and the formation of the endocardial cushions of the AVC. Our results also indicate that signaling through ALK3 is dispensable for hematopoiesis.

ALK3 in hematopoiesis

There is great interest in identifying inductive signals that initiate the hematopoietic program. *Xenopus* animal cap explants, avian, mouse ES/EB cell culture and knockout studies have suggested that members of TGFβ and fibroblast growth factor (FGF) families are crucial for hematopoietic development (Adelman et al., 2002; Chang et al., 1999; Dickson et al., 1995; Faloon et al., 2000; Flamme et al., 1995; Flamme and Risau, 1992; Huber et al., 1998; Johansson and Wiles, 1995; Kanatsu and Nishikawa, 1996; Liu et al., 2003; Maeno et al., 1996; Oshima et al., 1996; Pardanaud et al., 1996). Among the members of the TGFβ superfamily of growth factors, numerous studies indicate that BMP4 is important for hematopoietic development. We recently demonstrated that BMP4 is crucial for induction of brachyury$^+$ mesoderm from ES cells and FLK1$^+$ cells from brachyury$^+$ cells. In combination with VEGF, BMP4 significantly enhanced the production of SCL$^+$ hematopoietic cells (Park et al., 2004). Even though these studies suggested that BMP4 contributed to hematopoietic development, we could not position whether BMP4 functioned in the induction of FLK1$^+$ mesoderm or whether BMP4 was independently required for the induction of SCL$^+$ hematopoietic progenitors from FLK1$^+$ mesoderm. To further elucidate the function of BMP/BMP receptor-mediated signaling during the embryonic organogenesis, we generated *Alk3* CKO mice in which *Alk3* was inactivated in FLK1$^+$ cells. The analyses of *Alk3* CKO mutant yolk sacs and fetal livers indicated that blood cells developed normally in these mutants. Although we cannot exclude the possibility that other BMP type I receptors, such as ALK2 or ALK6, compensated for the loss of ALK3 activity, our studies provide genetic evidence that the BMP4-ALK3 axis is not crucial for hematopoietic development. Our observation is consistent with a recent study that hematopoietic development occurred normally in zebrafish when ALK3 signaling was blocked by an inducible dominant-negative ALK3 expression after the onset of gastrulation (Pyati et al., 2005).

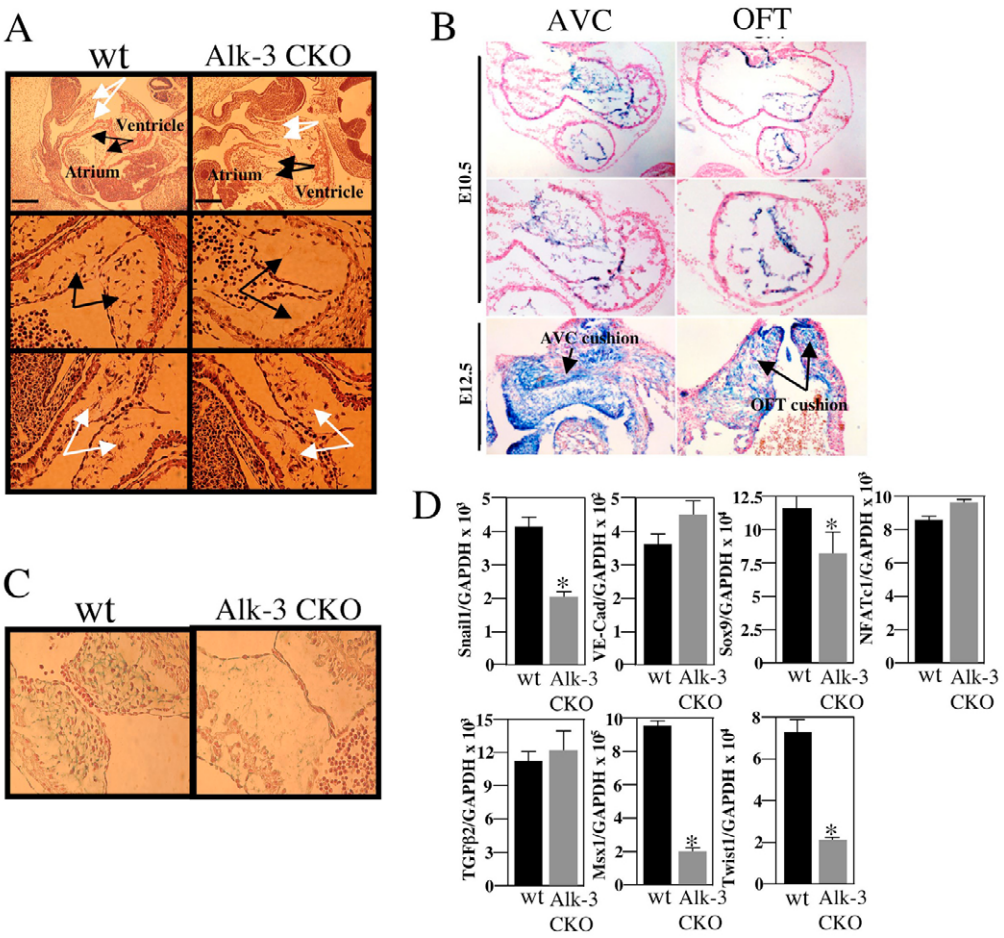

Fig. 6. The *Alk3* CKO embryos exhibit defects in the cushion formation in the AVC, but not in the OFT. (**A**) E10.5 wild-type (*n*=4) and *Alk3* CKO (*n*=4) embryos were sectioned sagittally and stained with Hematoxylin and Eosin. In the control (wild-type) embryos, trabeculae and endocardial cushions in the AVC region, as well as the OFT develop normally. The AVC cushion is missing in the *Alk3* CKO embryos, but the development of the OFT cushion persists. Black arrows and white arrows represent the cushion in the AVC and in the OFT, respectively. Middle and bottom panels represent higher magnification of the AVC and the OFT, respectively. Scale bars: 200 μm. (**B**) *Flk1*$^{+/Cre}$ mice were crossed with Rosa26R-*lacZ* mice and the resulting embryonic hearts were cross-sectioned, and subjected to *lacZ* staining. At E10.5, the majority of *lacZ*-positive cells in the AVC are present in the cushion cell layer and in the endocardium. However, in the OFT, the *lacZ*-positive cells are limited to the endocardium. By E12.5, all ACV cushion cells are *lacZ*$^{+}$, while the OFT cushion consists of both *lacZ*$^{+}$ and *lacZ*$^{-}$ cells. (**C**) Alcian Blue staining. (**D**) Quantitative RT-PCR analysis of E10.5 heart lacking the OFT and right ventricle for *Snai1*, VE-Cadherin (VE-Cad), *Sox9*, *Nfatc1*, *Tgfb2*, *Msx1 and Twist1*. Four wild-type and four mutant embryos were used for quantitative RT-PCR analysis. **P*<0.05.

The *Alk3* CKO hematopoietic phenotype suggested that non-BMP signaling, perhaps by signaling through TGFβ or activin receptors could contribute to hematopoietic cell development. *Tgfb1*$^{-/-}$ or *Tgfbr2*$^{-/-}$ mice show defects in yolk sac hematopoiesis, although *Tgfbr1*-deficient mice display enhanced hematopoiesis (Dickson et al., 1995; Larsson et al., 2001; Oshima et al., 1996). Additionally, activin A could increase hematopoietic development in the presence of BMP4 and VEGF (Park et al., 2004). To determine if any members of the TGFβ growth factor superfamily and their receptors are involved in hematopoietic specification, we analyzed hematopoietic development in the *Smad4* CKO embryos, and found that mutant embryos were morphologically normal at E8.5. However, E8.5 and E9.5 mutant yolk sacs contained one half as many hematopoietic progenitors as controls. This clearly indicates that SMAD4-dependent signaling contributes to the formation of hematopoietic cells from FLK1^{+} mesoderm.

Two groups reported that FGF receptor 1 null (*Fgfr1*$^{-/-}$) mice died in mid-gestation and displayed abnormal mesoderm patterning (Deng et al., 1994; Yamaguchi et al., 1994). Subsequently, we demonstrated that *Fgfr1*$^{-/-}$ ES cells differentiated up to the Brachyury^{+} cell stage but failed to express normal level of FLK1, suggesting a role for FGFR1 in the early stages of hematopoiesis (Faloon et al., 2000). Treatment of wild-type ES cells with FGF2, a ligand for FGFR1, enhanced the generation of FLK1^{+} cells (Faloon et al., 2000). To determine if the remaining hematopoietic activity in the *Smad4* CKO mutant is due to FGF signaling, we inactivated *Fgfr1* or *Fgfr1* and *Fgfr2* in FLK1^{+} cells. We found that *Fgfr1* CKO or *Fgfr1/2* double CKO mice were born alive and that E13.5 *Fgfr1/2* double CKO fetal liver contained similar levels of hematopoietic progenitors when compared with wild-type controls (see Fig. S2 in the supplementary material). Collectively, we conclude that FGF receptor signaling is required to generate FLK1^{+} mesoderm, but is

dispensable for subsequent hematopoietic development. In the future, the nature of the residual hematopoietic activity in *Smad4* CKO embryos still needs to be elucidated.

ALK3 in vessel development

Vessel formation in the developing embryo requires vasculogenesis and angiogenesis with successful recruitment of supporting cells such as smooth muscle cells (SMCs) and pericytes. Herein, we demonstrate that *Alk3* CKO embryos display defects in vessel remodeling, as well as vessel maturation/integrity. It is not clear why some of the mutants showed such a severe angiogenesis phenotype, while the remaining mutant embryos showed defects in vessel maturation and/or integrity. We suggest that it could be due to mixed genetic background or due to efficiency and/or timing of the recombination of *Alk3* floxed alleles. Nevertheless, *Alk3* CKO mutant embryos that died by E10.5 all formed a primary vascular plexus, but failed to complete angiogenesis. This observation provides the first genetic evidence that ALK3 is crucial for vessel remodeling. Our results are consistent with previous observations that BMP6 or BMP2 could promote endothelial tube formation and migration of endothelial cells in vitro (Langenfeld and Langenfeld, 2004; Valdimarsdottir et al., 2002). Activation of ALK3 induced tube formation and the migration of endothelial cells, in part, by stimulating the expression of *Id1* (Valdimarsdottir et al., 2002). Indeed, we found that expression of Id genes (*Id1-Id4*) was decreased by 40-60% in the mutant yolk sacs, compared with the controls. We propose that ALK3-mediated Id gene activation in endothelial cells is crucial for vessel remodeling in the yolk sac.

Alk3 CKO mutant embryos that died by E11.5 appeared to develop normal blood vessels in the yolk sac and in the embryo proper. Nonetheless, these mutants displayed dilated vessels in the brain and abnormal branching in the trunk and obvious vessel abnormalities when examined by TEM. The most striking phenotype was that all the *Alk3* CKO embryos showed abdominal hemorrhage by E11.5, suggesting that vessel integrity is defective. It has been reported that several pathways, including VEGF, PDGF/PDGFR, ANG1/TIE2 and ALK-1/endoglin have important functions in vessel integrity. PDGFB could recruit mural cells to endothelial cells (Hirschi et al., 1999), and mice lacking *Pdgfb* or *Pdgfrb* show a reduced degree of vascular SMCs and pericytes in vessels (Hellstrom et al., 1999; Lindahl et al., 1997). More recently, inactivation of *Pdgfb* in endothelial cells led to decreased recruitment of pericytes to vessels (Bjarnegard et al., 2004). In the present study, staining with antibodies to CD31 and SMC-α actin revealed that the endothelial cell layer in the dorsal aortas of *Alk3* CKO mutants was surrounded by a reduced number of SMCs. This observation was confirmed by TEM, which showed that SMCs in the *Alk3* CKOs did not make close contacts with endothelial cells. More importantly, we found frequent breaks in the endothelial cell layer on the dorsal aorta wall in the *Alk3* CKO mutants, while there were no obvious breaks found in the dorsal aorta of the controls. Expression of integrin αV and β3 was decreased in the mutants, although we did not find differences in angiopoeitin 1, angiopoeitin 2 and *Tie2* expression. Importantly, *Alk3* CKO embryos expressed decreased *Pten* with a concomitant increase in *Vegf* expression. There is emerging evidence that BMP signaling acts in the upstream of the PTEN/PI3K/VEGF pathway. Treatment of BMP2 can stabilize PTEN protein (Waite and Eng, 2003). Loss of *Alk3* not only results in the inhibition of PTEN activity, but also the activation of AKT, downstream of PI3K (He et al., 2004). PTEN can inhibit VEGF expression by inhibiting the PI3K/AKT pathway (Jiang et al., 2000; Pore et al., 2003). Furthermore, a recent study has demonstrated that abrogation of *Pten* in TIE2$^+$ cells leads to defects in angiogenesis and that these mutants display increased level of genes involved in vessel development including *Vegf* (Hamada et al., 2005). Collectively, we propose that ALK3 in FLK1$^+$ cells may regulate vessel integrity through the PTEN/PI3K/VEGF pathway.

As for SMC defects in *Alk3* CKO embryos, it is not clear whether the *Alk3* CKO vessel phenotype is due to *Alk3* deficiency in endothelial cells or whether SMC generation per se is defective. One possible explanation would be that *Alk3*-deficient endothelial cells fail to recruit SMCs to the dorsal aorta. However, we did not observe misplaced SMCs around the dorsal aorta. Furthermore, *Pdgfb* was equally expressed in wild-type and mutant dorsal aorta (not shown), although we cannot exclude the possibility that other pathways could be regulated by ALK3. Alternatively, absence of *Alk3* could lead to defective SMC generation, resulting in insufficient number of SMCs for vessel integrity. Indeed, we found decreased expression of SMC α-actin and myosin heavy chain in mutant dorsal aorta. Recent studies have shown that vascular endothelial cells or FLK1$^+$ endothelial cells can (trans)differentiate into SMCs during development (DeRuiter et al., 1997; Ema et al., 2003; Frid et al., 2002; Yamashita et al., 2000). Therefore, ALK3 could be required for SMC generation and/or transdifferentiation from endothelial cells.

Mice lacking *Tgfb1*, *Tgfbr1* (*Alk5*), *Alk1* or *Tgfbr2* all display varying degrees of yolk sac angiogenesis defects (Dickson et al., 1995; Larsson et al., 2001; Oh et al., 2000; Oshima et al., 1996). A similar phenotype has also been reported for *Smad5*$^{-/-}$ mice (Chang et al., 1999; Yang et al., 1999). Intriguingly, recent studies provide compelling evidence that ALK5 is exclusively expressed on SMCs (Seki et al., 2006). Thus, angiogenesis defects seen in *Alk5* mutant mice are most probably due to SMC defect indirectly affecting endothelial differentiation. Vessel remodeling and vessel maturation/integrity defects observed in *Alk3* CKO mutant mice are most similar to vessel abnormalities observed in *Alk1* knockout mice. Notably, mice deficient in *Alk1* showed dilated vessels. The *Alk1*-deficient dorsal aorta had significantly reduced levels of SMC (Oh et al., 2000), suggesting that a close interaction between endothelial cells and supporting cells is crucial for maintaining vessel integrity. Moreover, the expression of *Vegf*, *Plau1* and *Serpine1* was increased in both *Alk3* CKO and *Alk1* mutant mice. Additionally, all Id genes were downregulated in *Alk3* CKO mutants. As ALK1 mediated signals in endothelial cells were shown to activate Id genes (Goumans et al., 2002), it is of interest to see if *Id* gene expression is also downregulated in *Alk1* mutant mice. And yet, yolk sac vascular defects of *Alk1* knockout mice appear to be more severe compared with *Alk3* CKO embryos. For example, remodeling defects in *Alk1* knockout mice are obvious as early as E9.5, at which time point *Alk3* CKO embryos cannot be distinguished from the control embryos. To this end, it is important to note that all *Smad4* CKO embryos show angiogenesis defects. Collectively, we propose that vessel remodeling and maturation is achieved by redundant as well as specific signaling mediated by ALK1 versus ALK3.

ALK3 and AV cushion formation

One of the most distinct features of heart morphogenesis is an endothelial-mesenchymal transformation (EMT) (reviewed in Person et al., 2005). During this process, endocardium in the AVC and OFT differentiates into mesenchymal cells, are delaminated, and eventually invade the cardiac jelly, the extracellular matrix between the endocardium and the myocardium. The mechanisms involved in cushion formation or its further morphogenesis have been extensively studied. By using an in vitro explant culture system, it

has been shown that EMT could be induced by myocardium underlying the AVC (Mjaatvedt et al., 1987; Runyan and Markward, 1983). BMP2 and TGFβ2 could also induce EMT in endocardium explant culture (Sugi et al., 2004). Furthermore, *Tgfb2*$^{-/-}$ mice showed defects in the OFT, but initiation of endocardial cushion formation seemed to be normal (Sanford et al., 1997). Consistently, conditional inactivation of *Bmp2* in cardiomyocytes using the *Nkx2.5*-Cre system results in endocardial EMT defects (Ma et al., 2005). Conditional deletion of *Alk3* in cardiomyocytes using the *Mhc*-Cre system results in heart abnormalities involving the interventricular septum, trabeculae and AV cushion defects (Gaussin et al., 2002). In these mice, *Tgfb2* expression is greatly reduced, implying that TGFβ2 is crucial for AV cushion morphogenesis. Outflow tract defects are not observed in these mice. Intriguingly, conditional inactivation of *Bmp4* in cardiomyocytes using the *Nkx2.5*-Cre system results in defective outflow tract septation and abnormal morphogenesis of branchical arch arteries (Liu et al., 2004), while *Bmp4* inactivation using the rat troponin T (*Tnnt*)-Cre results in severe AVC defects (Jiao et al., 2003). Collectively, these studies emphasize the importance of myocardium in inducing EMT. It is important to note that *Alk3*-mediated signaling in the cardiomyocytes is important for myocardium proliferation and for AVC morphogenesis.

Herein, we demonstrate that ALK3 signaling in the endocardium is intrinsically required for AV cushion formation. The selective absence of the endocardial cushions in the AVC raised the issue of whether the origin of endocardium in the AVC is different from that of the OFT. However, we found that FLK1$^+$ cells can contribute to both AVC and OFT endocardial cushions. Given the finding that neural crest cells also contribute to the OFT, but not to the AV cushion (Epstein et al., 2000; Gitler et al., 2003), it is possible that ALK3 signaling in neural crest cells in the OFT rescued the *Alk3* deficiency in the FLK1$^+$ cells. Recently, Wang et al. (Wang et al., 2005) demonstrated that conditional inactivation of *Alk-2* using the *Tie-2*-Cre system resulted in selective defects in the AV superior cushion. The AV inferior cushion appeared to be normal in these mice. At E14.5, the surviving *Alk-2* CKO mutant embryos showed a range of ventricular septal defects. The differences in AV cushion defects observed in our studies compared with Wang et al. (Wang et al., 2005) could be due to the nature of cells that express Cre (FLK1$^+$ versus TIE2$^+$ cells). However, the specificity of the ALK2 versus ALK3 in superior versus inferior cushion formation cannot be ruled out. As for the timing of the *Alk3* inactivation, it is worth noting that about a third of *Alk3* conditional mutants using the *Tie2*-Cre system developed relatively normal AV cushion (Ma et al., 2005). Importantly, conditional inactivation of *Alk3* in neural crest cells using the *Wnt1*-Cre system results in outflow tract defects including a septal failure and reduced conotruncal length (Stottmann et al., 2004). Moreover, mice homozygous for a hypomorphic allele of *Bmpr2* displayed defects in the formation of the OFT valve, but the AVC cushion formation was normal, despite the ubiquitous expression of *Bmpr2* in the heart (Delot et al., 2003; Roelen et al., 1997).

During the AV cushion EMT, AV endocardium loses the characteristics of endothelial cells and cell-cell interaction, while activating genes for mesenchymal cells. *Snai1*, a Slug family member, and *Twist1*, a basic HLH transcription factor is known to promote the EMT by downregulating VE-cadherin and/or E-cadherin (Timmerman et al., 2004; Yang et al., 2004). We found a reduced expression level of *Snai1* and *Twist1* with sustained expression of VE-cadherin in *Alk3* CKO embryos. Inactivation of *Alk3* in *Tie2* Cre mice showed a loss of *Twist1* and a mild defect in VE-cadherin, although *Snail1* expression was not affected (Ma et al., 2005). SOX9, a high-motility group transcription factor, is expressed in the mesenchymal cells of AV and OFT cushion (Akiyama et al., 2004). SOX9 has been implicated in neural crest cell delamination and AVC cushion formation (Akiyama et al., 2004; Cheung and Briscoe, 2003). Conditional knockout of *Sox9* in the *Wnt1*-Cre system showed ectopic expression of *Nfatc1*, leading to a failure of cushion cell development (Akiyama et al., 2004). We observed that *Sox9* expression was downregulated, while *Nfatc1* expression was not affected in *Alk3* CKO hearts. These results suggest that ALK3 signaling in the AV endocardium is crucial for the initiation stage of the AV EMT. As Snail and Sox9 are important regulators of Notch and Wnt/β-catenin, respectively, it will be interesting to see if ALK3 signaling interacts with these pathways in the AV EMT. Collectively, we show that ALK3 signaling is required for the AV cushion formation. Further studies on redundant as well as distinct signaling mediated by ALK3 versus ALK2 are warranted.

We thank Thomas Sato for *Flk1*$^{+/Cre}$ mice; Darcy Gill for help with EM studies; Huiteng Cheng for help with embryo manipulation and discussion; James Richardson and Eric Olson for confirming the heart phenotype; and Robert Mecham, David Beebe and Choi laboratory members for helpful discussion. We also thank David Beebe and Jesse Lugus for critically reading the manuscript. This work was supported by grants from the National Institutes of Health, NHLBI, R01s HL63736 and HL55337 (to K.C.) and, in part, by the Intramural Research Program of the NIH, National Institute of Environmental Health Sciences (to Y.M.).

Supplementary material

Supplementary material for this article is available at http://dev.biologists.org/cgi/content/full/132/17/3473/DC1

References

Adelman, C. A., Chattopadhyay, S. and Bieker, J. J. (2002). The BMP/BMPR/Smad pathway directs expression of the erythroid-specific EKLF and GATA1 transcription factors during embryoid body differentiation in serum-free media. *Development* **129**, 539-549.

Akiyama, H., Chaboissier, M. C., Behringer, R. R., Rowitch, D. H., Schedl, A., Epstein, J. A. and de Crombrugghe, B. (2004). Essential role of Sox9 in the pathway that controls formation of cardiac valves and septa. *Proc. Natl. Acad. Sci. USA* **101**, 6502-6507.

Bjarnegard, M., Enge, M., Norlin, J., Gustafsdottir, S., Fredriksson, S., Abramsson, A., Takemoto, M., Gustafsson, E., Fassler, R. and Betsholtz, C. (2004). Endothelium-specific ablation of PDGFB leads to pericyte loss and glomerular, cardiac and placental abnormalities. *Development* **131**, 1847-1857.

Chang, H., Huylebroeck, D., Verschueren, K., Guo, Q., Matzuk, M. M. and Zwijsen, A. (1999). Smad5 knockout mice die at mid-gestation due to multiple embryonic and extraembryonic defects. *Development* **126**, 1631-1642.

Cheung, M. and Briscoe, J. (2003). Neural crest development is regulated by the transcription factor Sox9. *Development* **130**, 5681-5693.

Chung, Y. S., Zhang, W. J., Arentson, E., Kingsley, P. D., Palis, J. and Choi, K. (2002). Lineage analysis of the hemangioblast as defined by FLK1 and SCL expression. *Development* **129**, 5511-5520.

Delot, E. C., Bahamonde, M. E., Zhao, M. and Lyons, K. M. (2003). BMP signaling is required for septation of the outflow tract of the mammalian heart. *Development* **130**, 209-220.

Deng, C. X., Wynshaw-Boris, A., Shen, M. M., Daugherty, C., Ornitz, D. M. and Leder, P. (1994). Murine FGFR1 is required for early postimplantation growth and axial organization. *Genes Dev.* **8**, 3045-3057.

DeRuiter, M. C., Poelmann, R. E., VanMunsteren, J. C., Mironov, V., Markwald, R. R. and Gittenberger-de Groot, A. C. (1997). Embryonic endothelial cells transdifferentiate into mesenchymal cells expressing smooth muscle actins in vivo and in vitro. *Circ. Res.* **80**, 444-451.

Dickson, M. C., Martin, J. S., Cousins, F. M., Kulkarni, A. B., Karlsson, S. and Akhurst, R. J. (1995). Defective haematopoiesis and vasculogenesis in transforming growth factor-beta 1 knock out mice. *Development* **121**, 1845-1854.

Ema, M., Faloon, P., Zhang, W. J., Hirashima, M., Redi, T., Stanford, W., Choi, K. and Rossant, J. (2003). Combinatorial effects of Flk-1 and Tal1 (SCL) on vascular and hematopoietic development in the mouse. *Genes Dev.* **17**, 380-393.

Epstein, J. A., Li, J., Lang, D., Chen, F., Brown, C. B., Jin, F., Lu, M. M., Thomas, M., Liu, E., Wessels, A. et al. (2000). Migration of cardiac neural crest cells in Splotch embryos. *Development* **127**, 1869-1878.

Faloon, P., Arentson, E., Kazarov, A., Deng, C. X., Porcher, C., Orkin, S. and Choi, K. (2000). Basic fibroblast growth factor positively regulates hematopoietic development. *Development* **127**, 1931-1941.
Flamme, I. and Risau, W. (1992). Induction of vasculogenesis and hematopoiesis in vitro. *Development* **116**, 435-439.
Flamme, I., Breier, G. and Risau, W. (1995). Vascular endothelial growth factor (VEGF) and VEGF receptor 2 (flk-1) are expressed during vasculogenesis and vascular differentiation in the quail embryo. *Dev. Biol.* **169**, 699-712.
Frid, M. G., Kale, V. A. and Stenmark, K. R. (2002). Mature vascular endothelium can give rise to smooth muscle cells via endothelial-mesenchymal transdifferentiation: in vitro analysis. *Circ. Res.* **90**, 1189-1196.
Gaussin, V., Van de Putte, T., Mishina, Y., Hanks, M. C., Zwijsen, A., Huylebroeck, D., Behringer, R. R. and Schneider, M. D. (2002). Endocardial cushion and myocardial defects after cardiac myocyte-specific conditional deletion of the bone morphogenetic protein receptor ALK3. *Proc. Natl. Acad. Sci. USA* **99**, 2878-2883.
Gitler, A. D., Zhu, Y., Ismat, F. A., Lu, M. M., Yamauchi, Y., Parada, L. F. and Epstein, J. A. (2003). Nf1 has an essential role in endothelial cells. *Nat. Genet.* **33**, 75-79.
Goumans. M. J., Valdimarsdottir, G., Itoh, S., Rosendahl, A., Sideras, P. and ten Dijke, P. (2002). Balancing the activation state of the endothelium via two distinct TGF-beta type I receptors. *EMBO J.* **21**, 1743-1753.
Hamada, K., Sasaki, T., Koni, P. A., Natsui, M., Kishimoto, H., Sasaki, J., Yajima, N., Horie, Y., Hasegawa, G., Naito, M. et al. (2005). The PTEN/PI3K pathway governs normal vascular development and tumor angiogenesis. *Genes Dev.* **19**, 2054-2065.
He, X. C., Zhang, J., Tong, W. G., Tawfik, O., Ross, J., Scoville, D. H., Tian, Q., Zeng, X., He, X., Wiedemann, L. M. et al. (2004). BMP signaling inhibits intestinal stem cell self-renewal through suppression of Wnt-beta-catenin signaling. *Nat. Genet.* **36**, 1117-1121.
Hellstrom, M., Kalen, M., Lindahl, P., Abramsson, A. and Betsholtz, C. (1999). Role of PDGF-B and PDGFR-beta in recruitment of vascular smooth muscle cells and pericytes during embryonic blood vessel formation in the mouse. *Development* **126**, 3047-3055.
Hirschi, K. K., Rohovsky, S. A., Beck, L. H., Smith, S. R. and D'Amore, P. A. (1999). Endothelial cells modulate the proliferation of mural cell precursors via platelet-derived growth factor-BB and heterotypic cell contact. *Circ. Res.* **84**, 298-305.
Huber, T. L., Zhou, Y., Mead, P. E. and Zon, L. I. (1998). Cooperative effects of growth factors involved in the induction of hematopoietic mesoderm. *Blood* **92**, 4128-4137.
Huber, T. L., Kouskoff, V., Fehling, H. J., Palis, J. and Keller, G. (2004). Haemangioblast commitment is initiated in the primitive streak of the mouse embryo. *Nature* **432**, 625-630.
Jiang, B. H., Zheng, J. Z., Aoki, M. and Vogt, P. K. (2000). Phosphatidylinositol 3-kinase signaling mediates angiogenesis and expression of vascular endothelial growth factor in endothelial cells. *Proc. Natl. Acad. Sci. USA* **97**, 1749-1753.
Jiao, K., Kulessa, H., Tompkins, K., Zhou, Y., Batts, L., Baldwin, H. S. and Hogan, B. L. (2003). An essential role of Bmp4 in the atrioventricular septation of the mouse heart. *Genes Dev.* **17**, 2362-2367.
Johansson, B. M. and Wiles, M. V. (1995). Evidence for involvement of activin A and bone morphogenetic protein 4 in mammalian mesoderm and hematopoietic development. *Mol. Cell. Biol.* **15**, 141-151.
Kanatsu, M. and Nishikawa, S. I. (1996). In vitro analysis of epiblast tissue potency for hematopoietic cell differentiation. *Development* **122**, 823-830.
Langenfeld, E. M. and Langenfeld, J. (2004). Bone morphogenetic protein-2 stimulates angiogenesis in developing tumors. *Mol. Cancer Res.* **2**, 141-149.
Larsson, J., Goumans, M. J., Sjostrand, L. J., van Rooijen, M. A., Ward, D., Leveen, P., Xu, X., ten Dijke, P., Mummery, C. L. and Karlsson, S. (2001). Abnormal angiogenesis but intact hematopoietic potential in TGF-beta type I receptor-deficient mice. *EMBO J.* **20**, 1663-1673.
Lechleider, R. J., Ryan, J. L., Garrett, L., Eng, C., Deng, C., Wynshaw-Boris, A. and Roberts, A. B. (2001). Targeted mutagenesis of Smad1 reveals an essential role in chorioallantoic fusion. *Dev. Biol.* **240**, 157-167.
Lindahl, P., Johansson, B. R., Leveen, P. and Betsholtz, C. (1997). Pericyte loss and microaneurysm formation in PDGF-B-deficient mice. *Science* **277**, 242-245.
Liu, B., Sun, Y., Jiang, F., Zhang, S., Wu, Y., Lan, Y., Yang, X. and Mao, N. (2003). Disruption of Smad5 gene leads to enhanced proliferation of high-proliferative potential precursors during embryonic hematopoiesis. *Blood* **101**, 124-133.
Liu, W., Selever, J., Wang, D., Lu, M. F., Moses, K. A., Schwartz, R. J. and Martin, J. F. (2004). Bmp4 signaling is required for outflow-tract septation and branchial-arch artery remodeling. *Proc. Natl. Acad. Sci. USA* **101**, 4489-4494.
Ma, L., Lu, M. F., Schwartz, R. J. and Martin, J. F. (2005). Bmp2 is essential for cardiac cushion epithelial-mesenchymal transition and myocardial patterning. *Development* **132**, 5601-5611.
Maeno, M., Mead, P. E., Kelley, C., Xu, R. H., Kung, H. F., Suzuki, A., Ueno, N. and Zon, L. I. (1996). The role of BMP-4 and GATA-2 in the induction and differentiation of hematopoietic mesoderm in Xenopus laevis. *Blood* **88**, 1965-1972.
Mishina, Y., Suzuki, A., Ueno, N. and Behringer, R. R. (1995). Bmpr encodes a type I bone morphogenetic protein receptor that is essential for gastrulation during mouse embryogenesis. *Genes Dev.* **9**, 3027-3037.
Mishina, Y., Hanks, M. C., Miura, S., Tallquist, M. D. and Behringer, R. R. (2002). Generation of Bmpr/Alk3 conditional knockout mice. *Genesis* **32**, 69-72.
Mjaatvedt, C. H., Lepera, R. C. and Markwald, R. R. (1987). Myocardial specificity for initiating endothelial-mesenchymal cell transition in embryonic chick heart correlates with a particulate distribution of fibronectin. *Dev. Biol.* **119**, 59-67.
Morikawa, Y. and Cserjesi, P. (2004). Extra-embryonic vasculature development is regulated by the transcription factor HAND1. *Development* **131**, 2195-2204.
Motoike, T., Markham, D. W., Rossant, J. and Sato, T. N. (2003). Evidence for novel fate of Flk1+ progenitor: contribution to muscle lineage. *Genesis* **35**, 153-159.
Oh, S. P., Seki, T., Goss, K. A., Imamura, T., Yi, Y., Donahoe, P. K., Li, L., Miyazono, K., ten Dijke, P., Kim, S. et al. (2000). Activin receptor-like kinase 1 modulates transforming growth factor-beta 1 signaling in the regulation of angiogenesis. *Proc. Natl. Acad. Sci. USA* **97**, 2626-2631.
Oshima, M., Oshima, H. and Taketo, M. M. (1996). TGF-beta receptor type II deficiency results in defects of yolk sac hematopoiesis and vasculogenesis. *Dev. Biol.* **179**, 297-302.
Palis, J., Robertson, S., Kennedy, M., Wall, C. and Keller, G. (1999). Development of erythroid and myeloid progenitors in the yolk sac and embryo proper of the mouse. *Development* **126**, 5073-5084.
Pardanaud, L., Luton, D., Prigent, M., Bourcheix, L. M., Catala, M. and Dieterlen-Lievre, F. (1996). Two distinct endothelial lineages in ontogeny, one of them related to hemopoiesis. *Development* **122**, 1363-1371.
Park, C., Afrikanova, I., Chung, Y. S., Zhang, W. J., Arentson, E., Fong, G.-H., Rosendahl, A. and Choi, K. (2004). A hierarchical order of factors in the generation of FLK1- and SCL-expressing hematopoietic and endothelial progenitors from embryonic stem cells. *Development* **131**, 2749-2762.
Person, A. D., Klewer, S. E. and Runyan, R. B. (2005). Cell biology of cardiac cushion development. *Int. Rev. Cytol.* **243**, 287-335.
Pore, N., Liu, S., Haas-Kogan, D. A., O'Rourke, D. M. and Maity, A. (2003). PTEN mutation and epidermal growth factor receptor activation regulate vascular endothelial growth factor (VEGF) mRNA expression in human glioblastoma cells by transactivating the proximal VEGF promoter. *Cancer Res.* **63**, 236-241.
Pyati, U. J., Webb, A. E. and Kimelman, D. (2005). Transgenic zebrafish reveal stage- specific roles for Bmp signaling in ventral and posterior mesoderm development. *Development* **132**, 2333-2343.
Roelen, B. A., Goumans, M. J., van Rooijen, M. A. and Mummery, C. L. (1997). Differential expression of BMP receptors in early mouse development. *Int. J. Dev. Biol.* **41**, 541-549.
Runyan, R. B. and Markwald, R. R. (1983). Invasion of mesenchyme into three-dimensional collagen gels: a regional and temporal analysis of interaction in embryonic heart tissue. *Dev. Biol.* **95**, 108-114.
Ruzinova, M. B. and Benezra, R. (2003). Id proteins in development, cell cycle and cancer. *Trends Cell Biol.* **13**, 410-418.
Sanford, L. P., Ormsby, I., Gittenberger-de Groot, A. C., Sariola, H., Friedman, R., Boivin, G. P., Cardell, E. L. and Doetschman, T. (1997). TGFbeta2 knockout mice have multiple developmental defects that are non-overlapping with other TGFbeta knockout phenotypes. *Development* **124**, 2659-2670.
Seki, T., Hong, K. H. and Oh, S. P. (2006). Nonoverlapping expression patterns of ALK1 and ALK5 reveal distinct roles of each receptor in vascular development. *Lab. Invest.* **86**, 116-129.
Shalaby, F., Rossant, J., Yamaguchi, T. P., Gertsenstein, M., Wu, X. F., Breitman, M. L. and Schuh, A. C. (1995). Failure of blood-island formation and vasculogenesis in Flk-1-deficient mice. *Nature* **376**, 62-66.
Soriano, P. (1999). Generalized lacZ expression with the ROSA26 Cre reporter strain. *Nat. Genet.* **21**, 70-71.
Stottmann, R. W., Choi, M., Mishina, Y., Meyers, E. N. and Klingensmith, J. (2004). BMP receptor IA is required in mammalian neural crest cells for development of the cardiac outflow tract and ventricular myocardium. *Development* **131**, 2205-2218.
Sugi, Y., Yamamura, H., Okagawa, H. and Markwald, R. R. (2004). Bone morphogenetic protein-2 can mediate myocardial regulation of atrioventricular cushion mesenchymal cell formation in mice. *Dev. Biol.* **269**, 505-518.
Timmerman, L. A., Grego-Bessa, J., Raya, A., Bertran, E., Perez-Pomares, J. M., Diez, J., Aranda, S., Palomo, S., McCormick, F., Izpisua-Belmonte, J. C. et al. (2004). Notch promotes epithelial-mesenchymal transition during cardiac development and oncogenic transformation. *Genes Dev.* **18**, 99-115.
Tremblay, K. D., Dunn, N. R. and Robertson, E. J. (2001). Mouse embryos lacking Smad1 signals display defects in extra-embryonic tissues and germ cell formation. *Development* **128**, 3609-3621.
Valdimarsdottir, G., Goumans, M. J., Rosendahl, A., Brugman, M., Itoh, S., Lebrin, F., Sideras, P. and ten Dijke, P. (2002). Stimulation of Id1 expression

by bone morphogenetic protein is sufficient and necessary for bone morphogenetic protein-induced activation of endothelial cells. *Circulation* **106**, 2263-2270.

Waite, K. A. and Eng, C. (2003). BMP2 exposure results in decreased PTEN protein degradation and increased PTEN levels. *Hum. Mol. Genet.* **12**, 679-684.

Wang, J., Sridurongrit, S., Dudas, M., Thomas, P., Nagy, A., Schneider, M. D., Epstein, J. A. and Kaartinen, V. (2005). Atrioventricular cushion transformation is mediated by ALK2 in the developing mouse heart. *Dev. Biol.* **286**, 299-310.

Winnier, G., Blessing, M., Labosky, P. A. and Hogan, B. L. (1995). Bone morphogenetic protein-4 is required for mesoderm formation and patterning in the mouse. *Genes Dev.* **9**, 2105-2116.

Yamaguchi, T. P., Dumont, D. J., Conlon, R. A., Breitman, M. L. and Rossant, J. (1993). Flk-1, an flt-related receptor tyrosine kinase is an early marker for endothelial cell precursors. *Development* **118**, 489-498.

Yamaguchi, T. P., Harpal, K., Henkemeyer, M. and Rossant, J. (1994). fgfr1 is required for embryonic growth and mesodermal patterning during mouse gastrulation. *Genes Dev.* **8**, 3032-3044.

Yamashita, J., Itoh, H., Hirashima, M., Ogawa, M., Nishikawa, S., Yurugi, T., Naito, M., Nakao, K. and Nishikawa, S. (2000). Flk1-positive cells derived from embryonic stem cells serve as vascular progenitors. *Nature* **408**, 92-96.

Yang, J., Mani, S. A., Donaher, J. L., Ramaswamy, S., Itzykson, R. A., Come, C., Savagner, P., Gitelman, I., Richardson, A. and Weinberg, R. A. (2004). Twist, a master regulator of morphogenesis, plays an essential role in tumor metastasis. *Cell* **117**, 927-939.

Yang, X., Castilla, L. H., Xu, X., Li, C., Gotay, J., Weinstein, M., Liu, P. P. and Deng, C. X. (1999). Angiogenesis defects and mesenchymal apoptosis in mice lacking SMAD5. *Development* **126**, 1571-1580.

Yang, X., Li, C., Herrera, P. L. and Deng, C. X. (2002). Generation of Smad4/Dpc4 conditional knockout mice. *Genesis* **32**, 80-81.

Table S1. Genotypic analysis of pups from *Flk1*$^{+/Cre}$*Smad4*$^{+/floxed}$ × *Smad4*$^{floxed/floxed}$

	Flk1$^{+/Cre}$*Smad4*$^{floxed/floxed}$	*Flk1*$^{+/Cre}$*Smad4*$^{+/floxed}$	*Smad4*$^{floxed/floxed}$	*Smad4*$^{+/floxed}$
E8.5	4/15	5/15	4/15	2/15
E9.5	13(3*)/40	11/40	8/40	8/40
E10.5	1*/14	4/14	4/14	5/14
E11.5	3*/8	1/8	1/8	3/8

E, embryonic day; P, postnatal day; *, number of moribund embryos.